AAS 19-330

MISSION DESIGN FOR THE LUNAR PALLET LANDER

A. S. Craig*, J. P. Holt†, M. R. Hannan‡, and J. I. Orphee§

Marshall Space Flight Center is developing a small lunar lander capable of delivering up to 300 kg of payload to the lunar surface near the North or South Pole. Originally designed as a lander for a small rover, the Lunar Pallet Lander, has seen several design iterations over the last couple of years. This paper will cover how the vehicle and mission design changed from being a co-manifested payload candidate in NASA's Space Launch System to its current design, which could be launched with an Evolved Expendable Launch Vehicle (EELV), and reach a wide range of polar landing sites.

INTRODUCTION

Marshall Space Flight Center (MSFC) is developing a small lunar lander capable of delivering up to 300 kg of payload to the lunar surface near the North or South Pole. Originally designed as a lander for a small lunar rover, the Lunar Pallet Lander (LPL), has seen several design iterations over the last couple of years. This paper will cover how the vehicle and mission design changed from flying as a Space Launch System (SLS) co-manifested payload to its current design, which could be launched with an EELV class vehicle. The original concept of the lander was slated for an EELV launch; however the lander design was changed to accommodate a possible slot on the SLS Exploration Mission 2 flight. Later, it was finally decided that the lander should fly as a dedicated payload on an EELV, thus reverting to the original lander design concept. The ultimate objective of the LPL is to demonstrate autonomous precision landing capability on the Moon, allowing future landers and rovers to arrive very near to their target landing sites.

Early in the SLS Exploration Mission 2 (EM-2) mission design, the LPL, then known as Resource Prospector, was a leading candidate to fly as the co-manifested payload on the mission. That design utilized two ATK Star 37 Solid Rocket Motors (SRMs) in addition to the twelve 100-Lb hydrazine liquid-engine thrusters. The first SRM inserted the lander into a lunar orbit, while the second SRM provided the braking burn for the final descent to the surface. The targeted lunar orbit was 500 km above the mean surface with a near polar inclination. Due to the relatively large uncertainties in a SRMs performance, the orbit insertion cleanup was performed using the hydrazine thrusters. The parking orbit was required because as a Co-manifested Payload (CPL), the lander had no control on the launch date and it was required to land near a solstice, to maximize sun light for power generation. The descent used the liquid-engine thrusters to lower perilune to the desired altitude. Prior to perilune, the second Star 37 SRM would provide the bulk of the thrust for the braking burn, with the liquid-engine thrusters again cleaning up the maneuver and providing the impulse for the

*Aerospace Engineer, Guidance Navigation and Mission Design Branch, NASA, Marshall Space Flight Center.
†Pathways Intern, Guidance Navigation and Mission Design Branch, NASA, Marshall Space Flight Center.
‡Team Lead, Control Systems Branch, NASA, Marshall Space Flight Center.
§Aerospace Engineer, Guidance Navigation and Mission Design Branch, NASA, Marshall Space Flight Centers.

final descent. Both Star 37 motors could be stretched by up to 20% to provide the required impulse. The payload for that lander mission was a small lunar rover called Resource Prospector that needed to land at lunar dawn to maximize the daylight available, as the rover was powered by solar panels.

Not long after the initial mission design was completed, the SLS manifest changed and the LPL CPL slot was given to another payload. In addition, at about this time, the Resource Prospector mission was canceled, but the project continued the lander development with a dedicated launch vehicle and an arbitrary 300 kg lander payload. Flying on a dedicated vehicle provides more flexibility than flying on the SLS, because as a primary payload, the launch date can be set by the project and the need to wait in lunar orbit until a solstice is eliminated. To accommodate the new flight profile, the lander reverted to its original concept of using a single Star 48 SRM for a direct descent to the lunar surface. The Star 48 may be offloaded by up to 20%. However, to increase the number of possible landing sites on either pole of the Moon, many trajectories required a full use of the Star 48 SRM, with no offloading. Therefore, the intent is to design the trajectory so that the SRM will not require any offload. Once a landing site is selected for the mission, any excess SRM performance would be expended by using energy management maneuvers and/or biasing the SRM ignition times so that the burns are not fully optimal. Alternatively, while the size of the hydrazine tanks for the liquid engine thrusters are fixed, offloading hydrazine propellant is another option to improve performance. Thus, the final design of the vehicle uses a fully loaded Star 48 SRM to be robust enough to land at any possible landing site above 85 degrees north or south latitude, with preference toward landing at the lunar dawn for solar power reasons.

GENERAL MISSION DESIGN METHODOLOGY

The mission design will utilize Copernicus (Ref.1), an n-body trajectory optimization tool, developed and maintained at Johnson Space Center in Houston, TX. In recent years, the Copernicus developers have added a plugin capability (Ref.2 and 3) to the tool that allows a lot more flexibility. Specifically, the plugins were used to both approximate the launch vehicle's ascent to Low Earth Orbit (LEO) and to track the propellant utilization on the lander. The plugin to approximate the ascent calls a database of ascent trajectories that varies the insertion state as a function of launch azimuth as flown from either Kennedy Space Center (KSC) or Cape Canaveral Air Force Station (CCAFS), depending on the launch vehicle being examined. This database allows Copernicus to determine the time and LEO target inclination to optimize the lander's performance. The objective function for the analysis is to minimize the mission delta-V required of the lander with a maximum usable propellant constraint. The SRMs are only included in the objective function if they are being resized.

During the transit to the Moon, the lander will perform up to three Trajectory Correction Maneuvers (TCM's) to correct for launch vehicle errors and orbit perturbations. A total of 25 m/s has been set aside for these maneuvers, which is based on the LPL's mass just after launch vehicle separation, and 25 m/s is also consistent with other SLS missions. To assist with the navigation, state vector updates are planned to be uploaded to the lander sometime prior to each maneuver burn. Once the lander arrives in the vicinity of the moon, the mission profile changes depend on whether the LPL flies on SLS or an EELV.

For both launch vehicles, mission availability scans were run to show when the vehicle was capable of launching and achieving the desired landing site and time. The details of these scans will be discussed in the respective launch vehicle's section.

RESOURCE PROSPECTOR ON SLS BLOCK 1B

When MSFC initially started working on LPL it was being developed for Ames Research Center's (ARC) Resource Prospector rover that was being designed to test for volatiles near one of the lunar poles. The mission was one of several potential CPLs on the SLS EM-2 flight. For the original EM-2 Block 1B mission, as described in Reference 4, the Exploration Upper Stage (EUS) delivered the EUS/CPL)/Orion stack to a 100 nmi LEO. After anywhere from 120 to 176 minutes in LEO, the EUS re-ignited and performed an Apogee Raise Burn (ARB) to place Orion onto a 24-hour High Earth Orbit (HEO). Shortly after the ARB, the EUS/CPL stack and Orion separated. After separation (and approximately 30 minutes after the end of the ARB), the EUS performs the 1st (of two) Trans-Lunar Injection (TLI) burns, targeting the EUS/CPL stack to a lunar flyby for heliocentric disposal. After TLI-1, CPL separated from the EUS and re-targeted to an independent lunar arrival target. This profile was determined to be low risk to the Orion crew and offered the capability to send a multi-ton spacecraft to the lunar vicinity. Figure 1 provides an illustrative annotated graphic overview of the Block 1B Hybrid Free Return mission.

Figure 1. EM-2 on SLS Block 1B

A characteristic of using a circular parking orbit is the possibility for the launch vehicle to have multiple launch opportunities on each day. For the EM-2 mission profile, it meant that for many days there were two possible solutions, one on an ascending TLI and another on a descending TLI. The only reason there were not two opportunities on every day was due to the LEO coast constraints applied to the mission by both SLS (176 minute max) and Orion (120 minute minimum). The trend of launch opportunities can be see in Figure 2 where most days are viable except for 13 launch dates that violate the 120 minute minimum coast duration.

The landing sites for Resource Prospector were straightforward as ARC had already done a significant amount of work finding landing sites that where near permanently shadowed regions of the Moon that could hold water ice or other volatiles. These landing sites can be found in Table 1. The

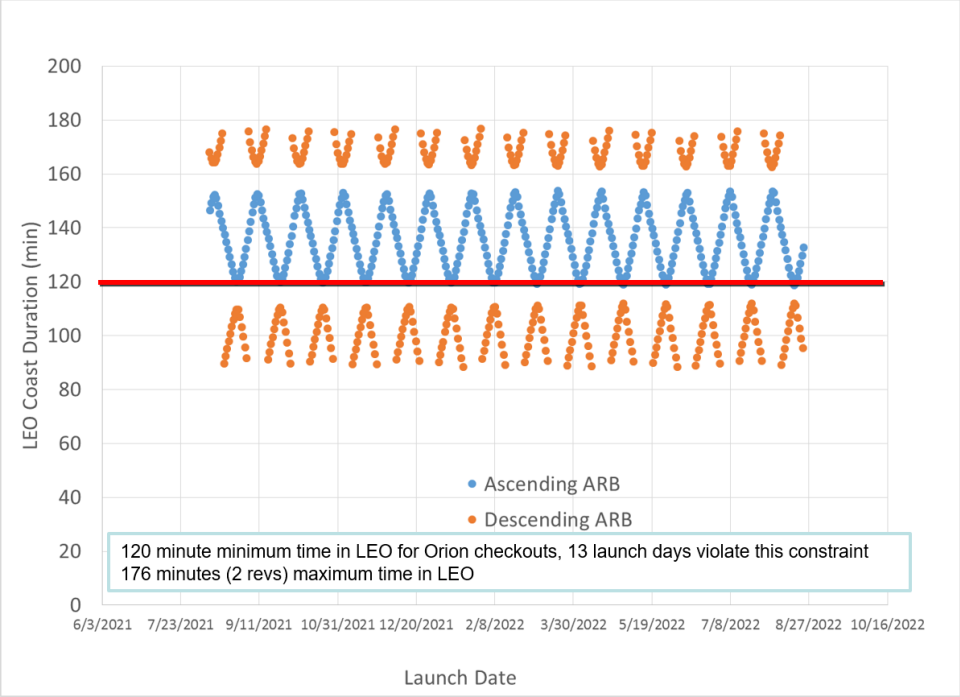

Figure 2. EM-2 Launch Availablility on SLS Block 1B

elevation is measured from the lunar reference radius of 1737.4 km. Since the SLS Block 1B was not planned to fly until at least 2021, the Erlanger landing site was discounted immediately as the Erlanger site required a landing date in 2020.

Table 1. Resource Prospector Landing Sites

Sites	Latitude (deg)	Longitude (deg)	Elevation (m)	Landing Time UTC
N. Shoemaker	-87.2407	59.1363	321.1781	1/18/2022 5:26:27 AM
N. Nobile	-85.0642	33.2857	5949.758	1/15/2022 2:50:58 PM
Hermite A.	86.6105	-45.7969	-259.7765	9/18/2021 7:44:18 AM
Erlanger	86.7532	30.7537	-569.8153	9/25/2020 6:59:20 PM

Resource Prospector Vehicle Configuration

The EM-2 launch date was being driven the SLS and Orion development schedules and the CPL had little say in what date the mission would launch. This meant that LPL had to loiter somewhere so that it would land at the desired time. To accommodate this mission profile, the configuration used two Star 37 SRMs to provide the bulk of the mission delta-V, and twelve 100 lbf liquid thrusters to provide cleanup maneuvers and the final descent. Twelve 5 lbf thrusters were also included for attitude control and small maneuvers.

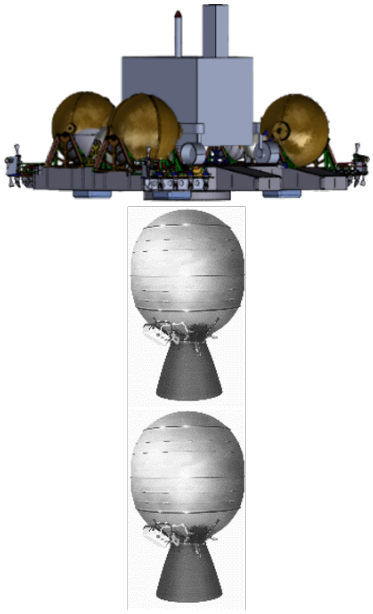

Figure 3. Resource Prospector Lander with 2 Star 37 motors

Resource Prospector Mission Profile

After the transit to the Moon and near perilune, the first Star 37 motor is fired to capture the lander into a near polar orbit at approximately 500 km altitude. As part of the optimization, the SRM was allowed to ”stretch” by up to 20% so that nominally, only one motor was required to insert into the desired orbit. To cover burn dispersions and orbit perturbations, some propellant was set aside for the liquid thrusters to perform a cleanup burn of up to 35 m/s. The mission delta V required through the lunar loiter was output from the 1 year trajectory scan, and can be seen in Figure 4. The 35 m/s was derived from this data based on the reference launch date of August 5, 2021 and the highest delta-V required from the scan. Propellant was also reserved for roll control during the SRM burn by assuming a 25%* duty cycle on the ACS. During the a lunar loiter of up to seven months, 20 m/s†was set aside to cover attitude control and orbit phasing to ensure the lander arrived to the landing site at the desired time. To assess if station keeping was required for this orbit, the trajectory was input into the General Mission Analysis Tool (GMAT) (Ref.5) and propagated over 6 months with varying degrees and order of the GRAIL (Ref.6) gravity model. The analysis showed that little to no station keeping would be required for a polar orbit as seen in Figure 5

Descent trajectories in Copernicus are best modeled backwards. That is, the analyst specifies the desired landing site and time in Copernicus and propagates backwards in time to find the required descent location from the lunar loiter orbit. To simplify this portion of the analysis, the descent was decoupled from the lunar orbit loiter and only required to start from a 500 km orbit. This allowed the two main legs of the mission to be optimized separately with the assumption that the orbit phasing could be introduced later. Only the lander’s mass was held continous between the two legs of the mission. For the purposes of the nominal mission profile, only 8 of the 12 main thrusters are used for optimization. This allows the other 4 to be used for off-pulsing for additional control authority or

*Placeholder number until more detailed analysis was available

†Placeholder number until more detailed analysis was available

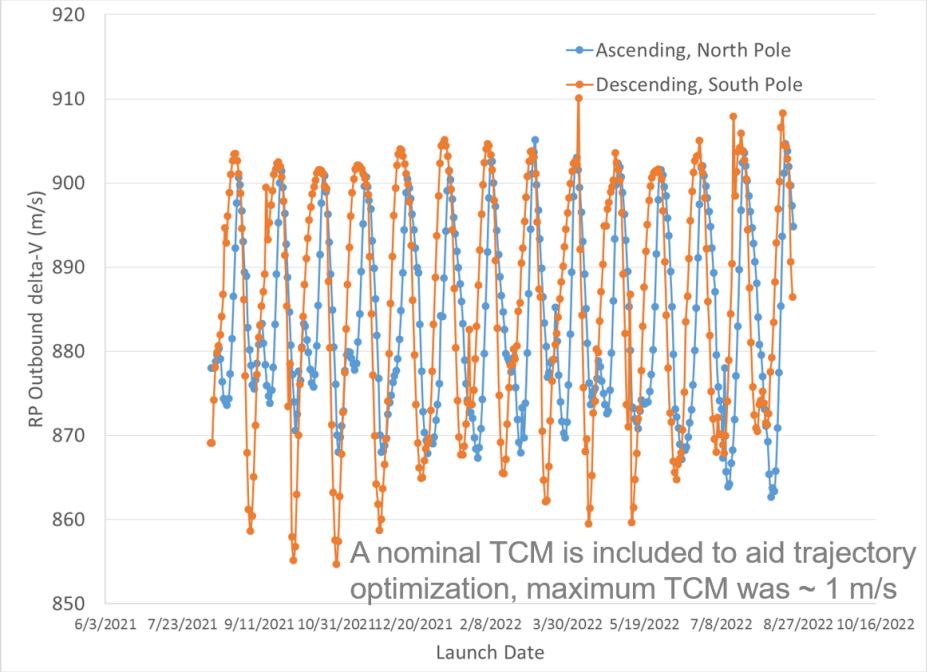

Figure 4. Mission Delta-V through Lunar Orbit Insertion

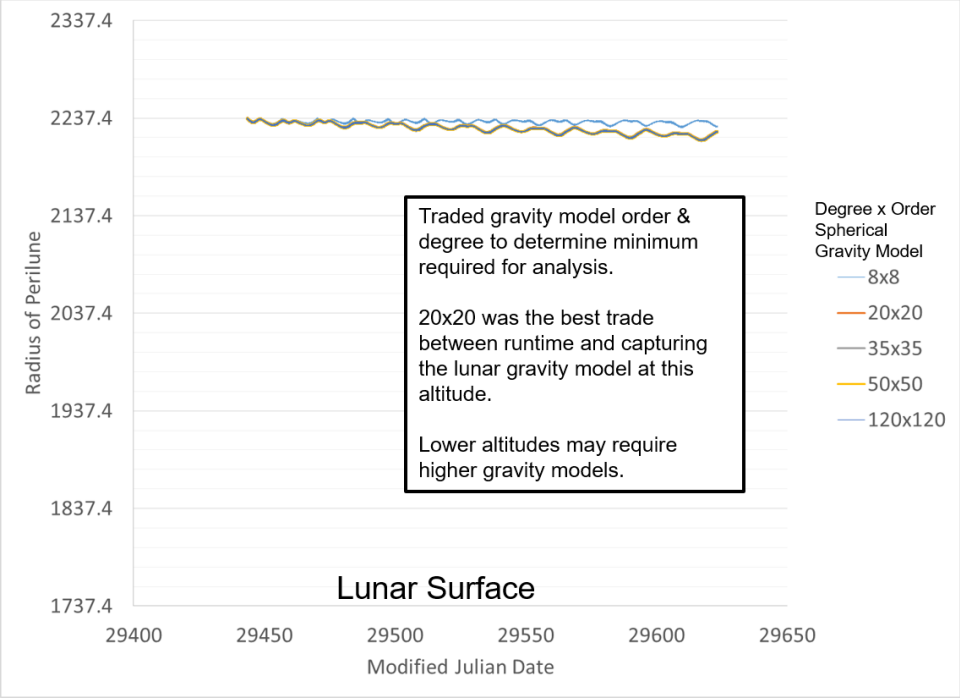

Figure 5. 500 km Lunar Polar Orbit Station Keeping

if additional thrust is needed to redirect the lander to the launch site due to large system dispersions after the final SRM burnout. Off-pulsing is commanding a one or multiple thrusters off for several milliseconds and is described in detail in Reference 7

While the descent is optimized backwards in time, it is easier to express the mission profile with time flowing forward. Starting from the loiter orbit, at an optimized time, the main thrusters are fired to bring the perilune down close to the lunar surface. The lander then coasts approximately half a revolution before the second Star 37 is fired. This kills the majority of the tangential velocity, leaving mostly radial velocity. Three different trajectories for the Star 37 were optimized simulataneously to model the effects of temperature dispersions on the SRM. The effects of three SRM temperatures can be seen graphically in Figure 6. Once the Star 37 burn is complete, it separates from the lander and the lander will coast for approximately 20 seconds before it reorients to its desired liquid-engine burn attitude for the final descent. The final descent is broken into 3 phases. The first phase, a liquid-engine burn, occurs after a short coast at the end of the SRM burnout. A second phase turns the vehicle to be descending purely vertical. Finally, the last phase brings the lander downward velocity to about 1 m/s at 1 m above the surface.

The next phase of analysis was to link up the LOI to DOI to model the phasing required to get to the desired landing site, but the decision was made to not fly LPL on SLS before the phasing analysis could be completed.

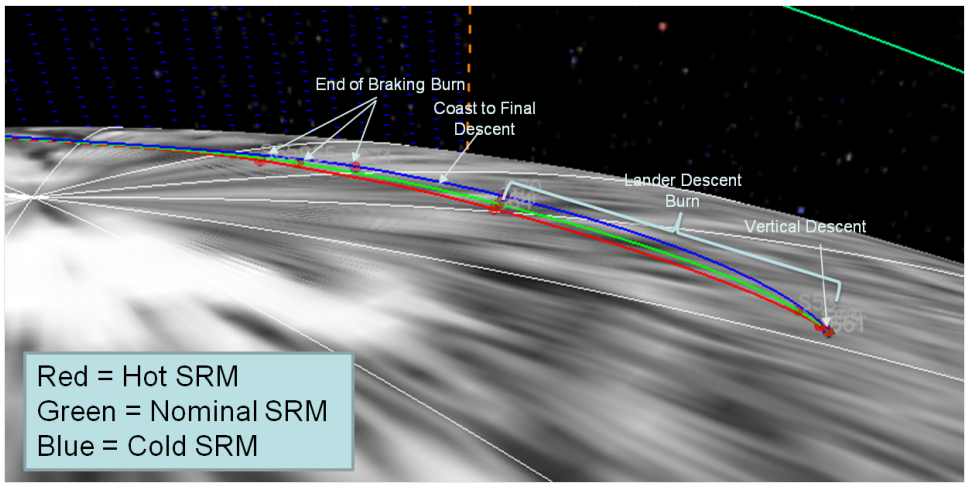

Figure 6. Resource Prospector Final Descent with SRM Temperature Dispersions

LUNAR PALLET LANDER ON AN EELV CLASS VEHICLE

Even though LPL was no longer a payload on an SLS mission, the development continued with a plan to fly as a primary payload on an EELV class vehicle in 2022. One of the chief benefits of being a primary payload is the mission design is greatly simplified. Instead of first inserting into a lunar loiter orbit; the lander will instead fly to a direct descent to the lunar surface. This change also necessitated reverting the configuration back to a single Star 48 SRM. The larger motor reduces the lunar relative velocity sufficiently so that the liquid thrusters can complete the descent.

While LPL was no longer associated with a specific science mission, the program continued designing the lander to accommodate an arbitrary 300 kg payload that could either be affixed to the

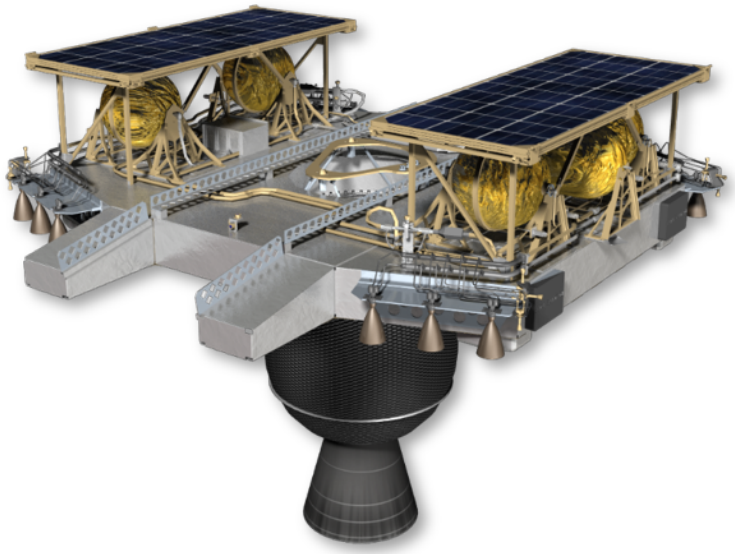

Figure 7. Lunar Pallet Lander with one Star 48AV motor

lander or be some form of lunar rover. Also, instead of specific landing sites near the lunar pole, the intent is to design the lander to land just about anywhere near the lunar poles. This required a change in tactics for the analysis. Instead of a handful of landing sites, scans of landing sites near the poles were required to show that LPL had the desired mission flexibility.

Another change was to attempt to bias the nominal descent trajectory for additional dispersions on the SRM burn. Analysis performed by Draper Labs several years prior (Ref.8) showed that the expected state error in the SRM burnout could be approximated by a 6 km downrange and 6 km crossrange error. The nominal trajectory was biased by including four additional descent trajectories that started from these +/- 6km errors in crossrange and downrange. This can be seen graphically in Figure 8. Each of the 5 trajectory legs required differing amounts of propellant, so the highest propellant consumption was preserved on the nominal mission leg by adding the excess propellant to the FPR. Typically, this was driven by the minimum downrange trajectory. Another change was the increase to using ten 100 lbf thrusters on the nominal trajectory instead of just eight. Analysis by the Guidance Navigation and Controls (GNC) team showed that less off-pulsing was needed that originally thought, so more thrusters were allocated to the nominal mission profile.

Some other key ground rules and assumptions that were updated included:

- A fixed FPR of 37.6 kg, updated from the original assumption of 2.5% of the loaded propellant
- The lander mass, including payload, was updated to 1264 kg
- Attitude control was estimated by burning six 5 lbf thrusters whenever the main thrusters are burning
- The Star 48AV will be used, which includes thrust vectoring, so only roll control is required during the solid burn. The 25% duty cycle on ACS for roll control remains.
- After some preliminary analysis, the team chose to ”fix” the Star 48 propellant to the full amount. The motor can be offloaded up to 20% of its propellant weight, but to improve landing site

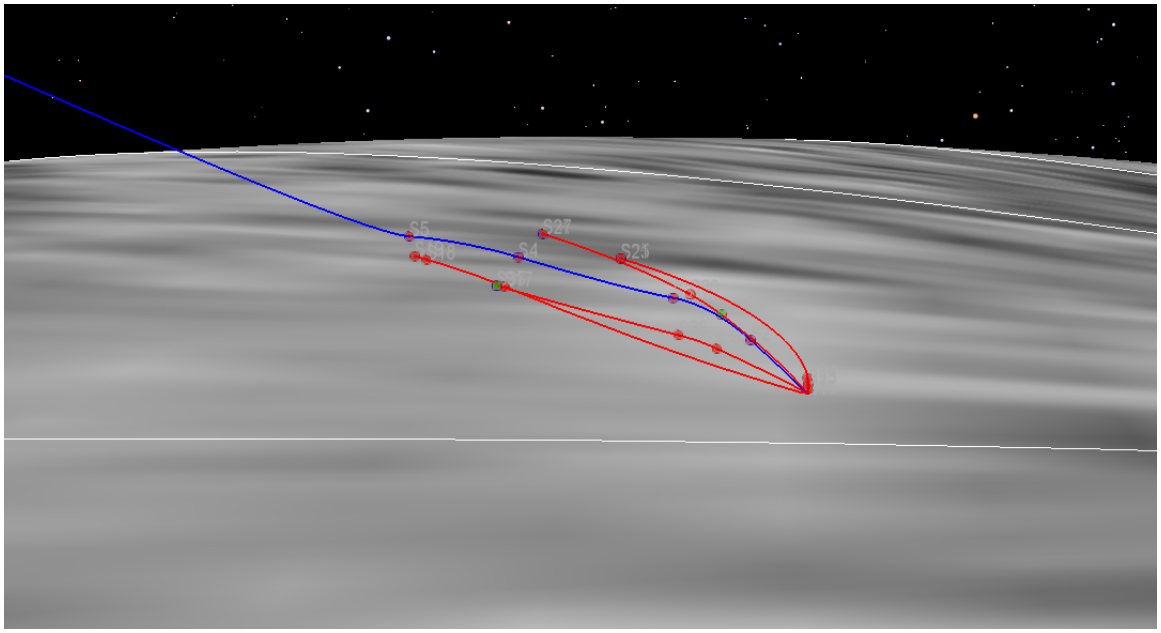

Figure 8. LPL Nominal trajectory in blue with the post-SRM dispersed trajectories in red

coverage, a full SRM would be required. The trajectory scans verified this assumption.

Modeling the Ascent without an Assigned Vehicle

When LPL was manifested on the SLS, existing trajectory data allowed to accurately model the ascent to TLI phase of the mission. However, until an EELV is selected, the ascent phase of the mission is approximated and an impulsive delta-V's is assumed for the TLI burn. The ascent was modeled in Copernicus by finding an insertion state 4600 km downrange from Cape Canaveral Air Force Station (CCAFS) to a 185 km circular orbit that flew over CCAFS. This downrange was estimated from SLS Block 1 and Block 1B trajectories and is only meant as a first order estimate until LPL has identified an acceptable launch vehicle. The states are meant to be generic, but modeling the ascent in this manner allows the analysis to more accurately estimate the outbound trajectory to the moon from LEO and to provide estimates on the TLI delta-V required to fly the mission on a given day. The insertion states were output as body fixed states and Copernicus used spline interpolation between the states to find the optimal launch azimuth for a given flight day. Launch azimuth is estimated using spherical trigonometry Eq. (1) (Ref.9) assuming the launch site is exactly at 28.5 degrees geocentric latitude. The states can be found in Table 2.

$$cos(inclination) = sin(azimuth) * cos(latitude) \tag{1}$$

Derivation of the Landing Sites

An optimal landing site is constrained as being located at lunar dawn, while also having line of sight of the Earth. To obtain a list of regions that fit this criterion, Systems Toolkit (STK) was first used to find the latitude and longitude of the Sun and Earth subpoints relative to the lunar surface, an example shown in Figure 9. Lunar dawn occurs close to the lunar terminator, which is offset

Table 2. Launch Vehicle Insertion States

Launch Azimuth (deg)	Inclination (deg)	Geodetic Altitude (km)	Longitude (deg)	Geodetic Latitude (deg)	Relative Velocity (km/s)	Flight Azimuth (deg)	Flight Path Angle (deg)
60.65	40	194.06	-31.88	40.18	7.43	89.33	0.00
62.17	39	193.69	-31.88	39.18	7.42	90.52	0.00
63.72	38	193.32	-31.91	38.15	7.42	91.73	0.00
65.33	37	192.94	-31.96	37.09	7.41	92.96	0.00
67.01	36	192.48	-32.05	35.81	7.41	95.76	0.00
68.77	35	192.14	-32.16	34.82	7.40	95.55	0.00
70.62	34	191.71	-32.32	33.60	7.40	96.93	0.00
72.61	33	191.27	-32.51	32.30	7.39	98.40	0.00
74.79	32	190.80	-32.77	30.88	7.39	99.98	0.00
77.26	31	190.28	-33.11	29.28	7.38	101.75	0.00
80.21	30	189.69	-33.57	27.38	7.38	103.86	0.00
84.40	29	188.92	-34.33	24.73	7.38	106.79	0.00
90.00	28.5	187.74	-35.93	20.24	7.37	111.85	0.00
95.60	29	187.13	-37.08	17.53	7.38	114.97	0.00
99.79	30	186.63	-38.28	15.05	7.38	117.90	0.00
102.74	31	186.33	-39.19	13.32	7.39	120.00	0.00
105.21	32	186.10	-40.00	11.90	7.39	121.77	0.00
107.39	33	185.93	-40.75	10.66	7.40	123.34	0.00
109.38	34	185.78	-41.46	9.54	7.40	124.78	0.00

approximately 89.6 degrees along the great circle from the Sun subpoint. Knowing the latitude and longitude of the sun subpoint, the longitude of the terminator λ_{term} can be found as a function of latitude φ_{term} using Eq. (2).

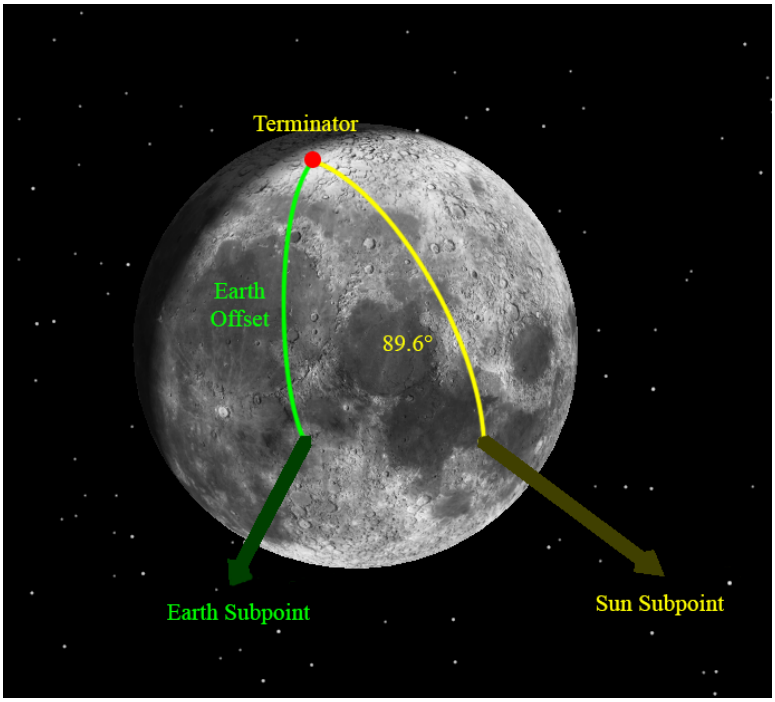

Figure 9. Sun and Earth subpoints relative to the lunar surface

$$\lambda_{\text{term}} = -acos[cos(89.6^{\text{o}})/(cos(\varphi_{\text{sun}})cos(\varphi_{\text{term}})] - tan(\varphi_{\text{sun}})tan(\varphi_{\text{term}})) + \lambda_{\text{sun}} \quad (2)$$

To filter out regions where the Earth is not visible, the great circle angle between the terminator and the earth subpoint is found using Eq. (3). If this angle is greater than 90 degrees, then the Earth is below the horizon and will not be visible. This is a simplifying assumption made for the purpose of sizing LPL. When a payload is identified, the desired landing sites will be screened using full lunar terrain data to guarantee line of site with Earth.

$$\theta = acos[sin(\varphi_{\text{earth}})sin(\varphi_{\text{term}}) + cos(\varphi_{\text{earth}})cos(\varphi_{\text{term}})cos(\lambda_{\text{term}} - \lambda_{\text{earth}})] \quad (3)$$

The regions from 85 to 88 degrees and from -85 to -88 degrees were studied. Using a 6-hour time step, the months of June and December 2022 were analyzed. A plot of suitable landing sites was created, as shown in Figure 10. Locations where the Earth offset angle is greater than 90 degrees are shown in red, with dark green representing the lowest Earth offset angle of 79 degrees. An example of a trajectory to one of the feasible landing sites with line of sight to Earth can be seen in Figure 11.

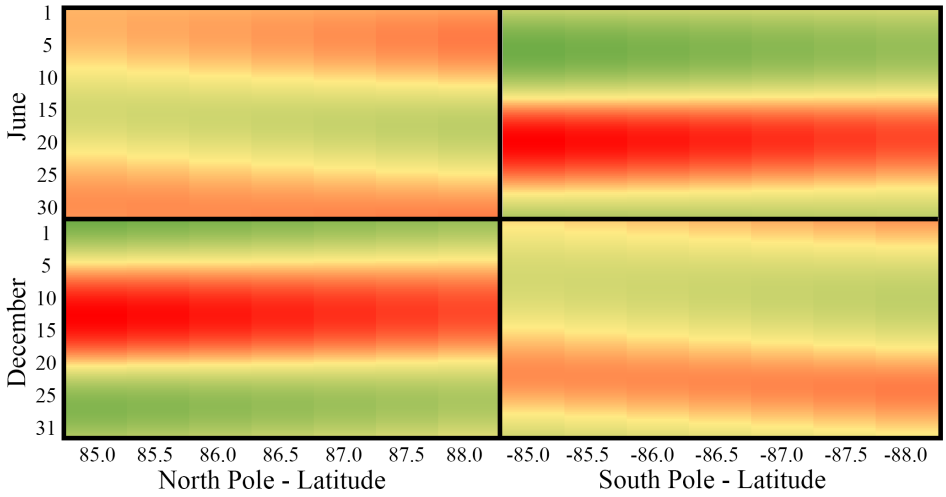

Figure 10. Earth offset angle from the lunar terminator as a function of latitude and time

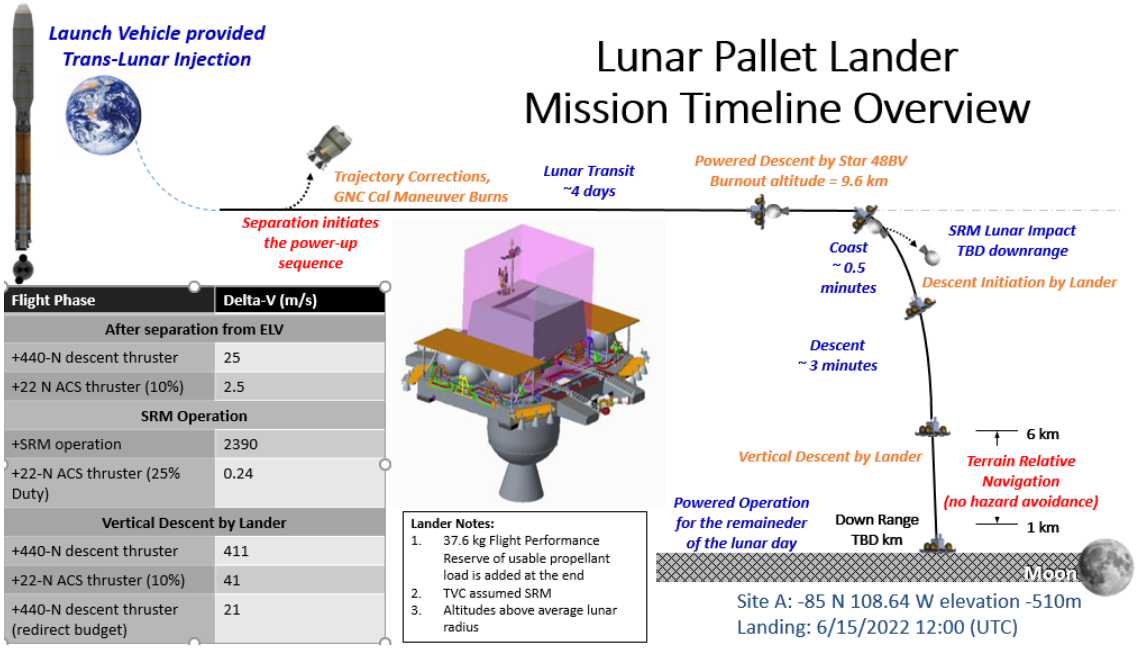

Flight Phase	Delta-V (m/s)
After separation from ELV	
+440-N descent thruster	25
+22 N ACS thruster (10%)	2.5
SRM Operation	
+SRM operation	2390
+22-N ACS thruster (25% Duty)	0.24
Vertical Descent by Lander	
+440-N descent thruster	411
+22-N ACS thruster (10%)	41
+440-N descent thruster (redirect budget)	21

Figure 11. Lunar Pallet Lander Mission Timeline to a Representative Landing Site

Landing Site Scans

Due to lighting conditions, the program decided to only fly to the north pole in June 2022 and south pole in December 2022.

Starting with the June 2022 landing sites at the north pole, a trajectory scan was run for one landing per day for the latitudes from 85 up to 88 degrees at 0.5 degree increments. Each landing site was at lunar dawn, which determined the landing site's longitude as described in the previous section. The results of the June 2022 scan showed that LPL had the capability to reach a landing site at least once per day for the region examined as see in in Figure 12. There appears to be a correlation between the landing site's altitude and the propellant remaining above the lander's FPR, Figure 13. This is most likely due to the >10 km altitude constraint at SRM burnout. This constraint was applied to keep the lander high above the lunar terrain to avoid mountains, but can be relaxed when the full terrain data is added.

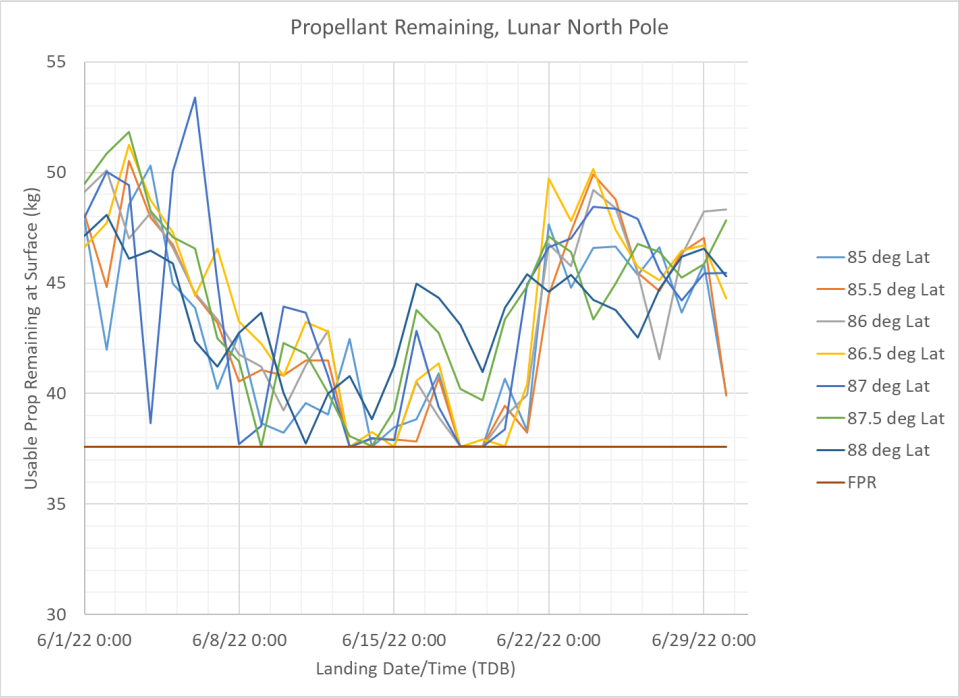

Figure 12. June 2022 Nominal Usable Propellant Remaining vs Landing Date/time

Similarly, the December 2022 landing sites were run showing that LPL was also capable of reaching a landing site at the Moon at least once per day. Figure 14 shows the results of the December scan, however, there were 3 landing sites that LPL could not reach. Two were very low in altitude (-5 and -4 km in altitude), which looking at the altitude trends in Figure 15, indicates that these sites may not be feasible with the current mission design. It may be possible to achieve the low altitude landing sites by lowering the SRM burnout altitude constraint, but that requires detailed terrain modeling, planned for a future phase of the analysis. The third non-reachable landing site is most likely due to an optimization error, as its altitude was high enough, at -2 km, that it should not have been a problem for the lander to arrive there. More analysis is required to verify this observation.

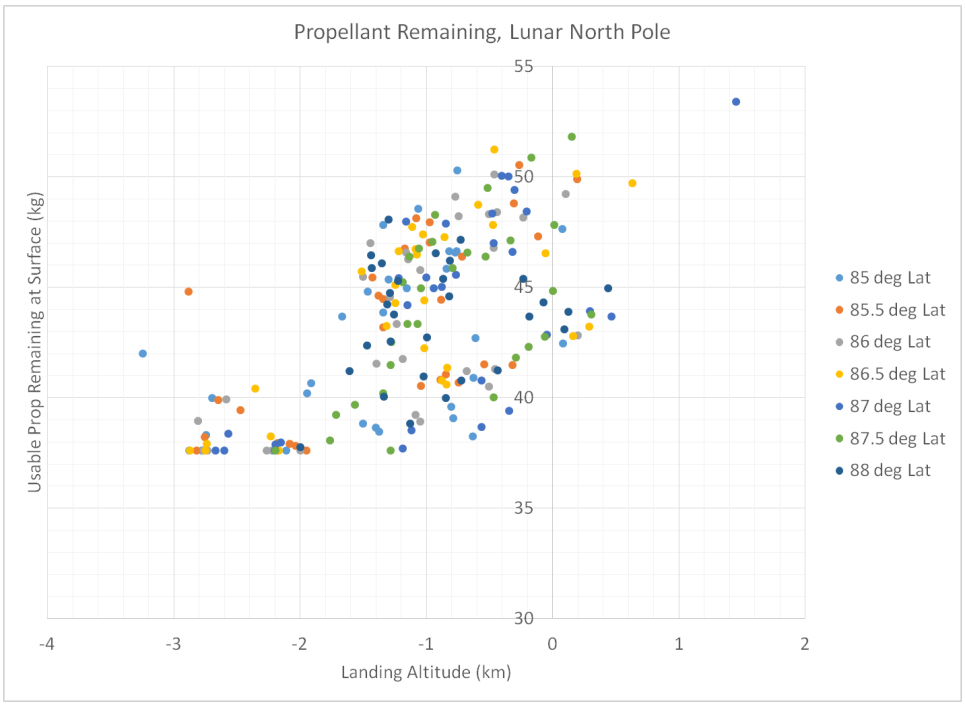

Figure 13. June 2022 Nominal Usable Propellant Remaining vs Altitude

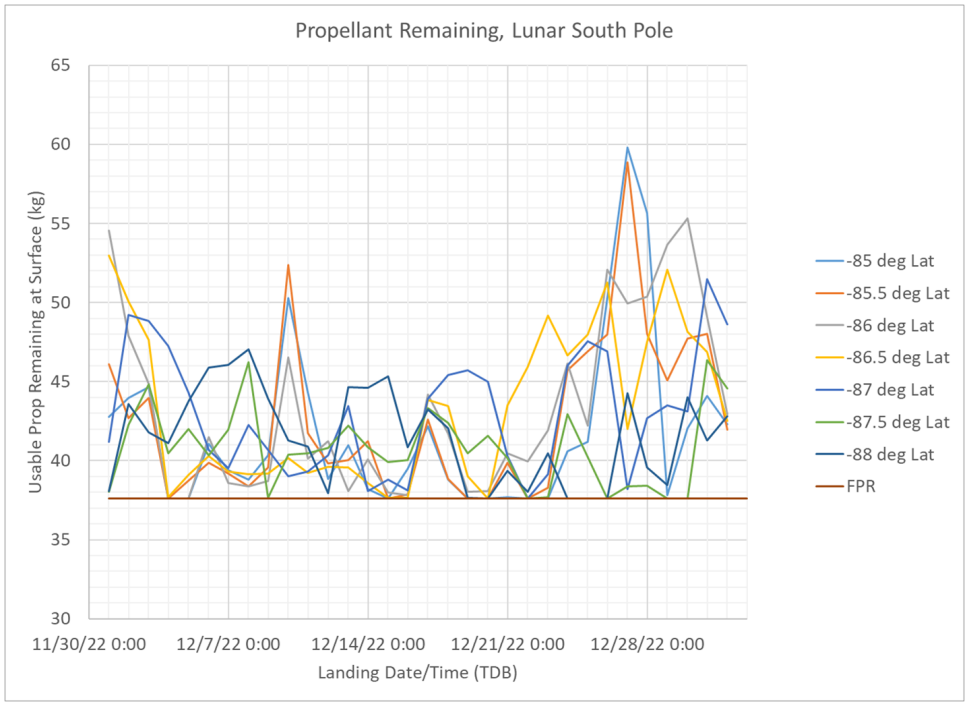

Figure 14. June 2022 Nominal Usable Propellant Remaining vs Landing Date/time

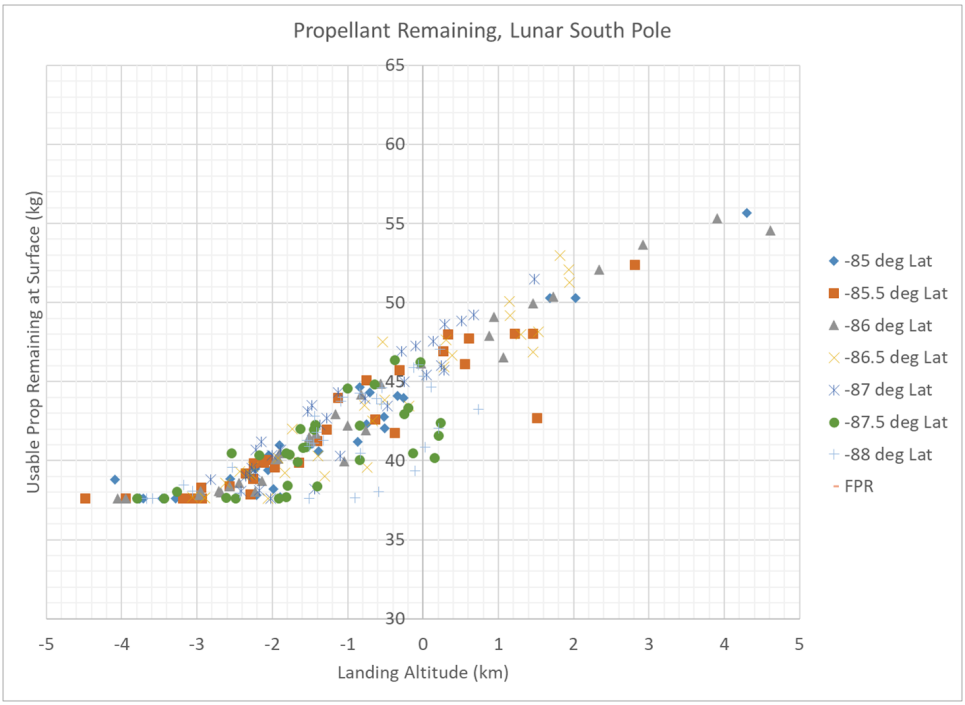

Figure 15. June 2022 Nominal Usable Propellant Remaining vs Altitude

ACKNOWLEDGMENTS

The authors would like to thank David Lee at JSC for providing the initial Copernicus idecks for the analysis when MSFC was first picking up this design. His work on an early iteration of the Resource Prospector lander still lingers on in the structure of the current idecks.

REFERENCES

[1] J. Williams, *Copernicus Version 4.6 Users Guide*. NASA Johnson Space Center, April 2018.

[2] J. Williams, "A New Architecture for Extending the Capabilities of the Copernicus Trajectory Optimization Program," *Advances in the Astronautical Sciences: Astrodynamics 2015*, Vol. 156, 2016. AAS 15-606.

[3] R. Whitley, J. Williams, J. Gutkowski, S. Craig, T. Dawn, C. Ocampo, B. Stein, D. Litton, R. Lugo, and M. Qu, "Combining Simulation Tools for End-to-End Trajectory Optimization," AAS/AIAA Astrodynamics Specialist Conference, August 2015. AAS 15-662.

[4] A. S. Craig, C. F. Berry, E. L. Christiansen, G. L. Condon, C. Foster, A. R. Harden, J. K. Little, T. Perryman, and S. B. Thompson, "NASA Exploration Mission 2 Mission Design," AAS/AIAA Space Flight Mechanics Meeting, January 2019. AAS 19-331.

[5] *General Mission Analysis Tool User Guide*. GMAT Development Team, 2018. http://gmat.sourceforge.net/docs/R2018a/html/index.html.

[6] *Gravity Recovery and Interior Laboratory*. PDS Geosiences Node, Washington University in St. Louis. http://pds-geosciences.wustl.edu/missions/grail/default.htm.

[7] M. Hannan, J. Orphee, and e. al, "Guidance, Navigation, and Control for the NASA Lunar Pallet Lander," AAS Guidance, Navigation and Control Conference, Feb. 2019. forthcoming.

[8] J.-W. Jang, S. Bhatt, M. Fritz, D. Woffinden, D. May, E. Braden, and M. Hannan, "Linear Covariance Analysis for a Lunar Lander," AIAA Guidance, Navigation, and Control Conference, AIAA SciTech Forum, 2017. AIAA-2017-1499.

[9] R. R. Bate, D. D. Mueller, and J. E. White, *Fundamentals of Astrodynamics*. 180 Varick Street, New York, NY 10014: Dover Publications, Inc, 1971.